

## A method of calculating ice loads when ice piles up on a fixed wall<sup>☆</sup>

A.V. Marchenko

*Moscow*

Received 9 November 2004

---

### Abstract

A model for calculating ice loads on a shelf ice-resistant platform is developed which corresponds to a cyclic scenario of the interaction of ice with the wall of a platform observed in laboratory experiments. Using relations which follow from the laws of conservation of mass, momentum and energy written for ice which fills a ridge formed at the wall of the platform, an explicit formula is obtained for the ice load on the wall. The generalized forces characterizing the dependence of the energy dissipation accompanying ridging on the dimensions of the sail and keel of the ridge and on the shape of the wall are parametrized. It is shown that the calculated loads obtained using the assumption of hydrostatic equilibrium of the sail and the keel of the ridge correspond to the lower boundary of the experimentally measured loads. The calculated loads obtained using the assumption that the keel of a ridge is of constant size yield an upper estimate of the ice loads. In order to estimate the limit loads at which collapse of the ice into the water occurs, a problem on the formation of a flexural crack in an ice floe which is thrust onto the wall is considered. The average and maximum ice loads on the wall of a platform are calculated on a real scale.

© 2006 Elsevier Ltd. All rights reserved.

---

When a platform standing on sealed interacts with a drifting ice cover, piling up of the ice occurs (or a ridge is formed) close to the platform. An estimate of the ice loads on the platform during the formation of the ridge is required when planning the conditions under which the platform is used and in order to avert catastrophes associated with the onset of high loads. A ridge consists of ice blocks which have been formed during the breakup of the edge of an ice field which is thrust onto a platform. As a rule, the characteristic size of the blocks varies from one to several metres and the thickness of the blocks is the same as that of the ice field. The horizontal and vertical dimensions of a ridge can reach several ten of metres, the extent of a ridge along the line of contact with a platform is of the order of the horizontal dimension of the platform at water level ( $\sim 100$  m) and the number of blocks of ice filling the vertical section of a ridge is of the order of hundreds. The direct use of models of continuum mechanics and granular media to model ridges is not physically justified if an ice block is assumed to be an analogue of a particle of a granular medium. In this sense the modelling of a ridge by discrete particles is more realistic (see Ref. 1, for example). At the same time, it is of interest to obtain analytical relations which enable one to estimate ice loads using traditional methods of continuum mechanics and without carrying out complex calculations.

A scheme of forces, which determine the overall load from the piling up of ice on a structure, was formulated and an empirical formula for calculating an ice load was proposed in Ref. 2. A method for calculating the stresses which arise

---

<sup>☆</sup> *Prikl. Mat. Mekh.* Vol. 70, No. 3, pp. 427–439, 2006.

*E-mail address:* [amarch@orc.ru](mailto:amarch@orc.ru).

during the formation of the ridge accompanying the compression of ice fields was developed in Ref. 3. In this approach, the relations between the stresses and strains follow from the laws for the conservation of the mass, momentum and energy of the broken ice filling a ridge. An expression for the dissipation of energy, which is determined by the scenario of the ice ridge build up, plays a key role. In this paper, this method is used to calculate the stresses accompanying the ridging of ice near a fixed wall.

### 1. Governing basic equations

The motion of a floating ice floe against a fixed wall is accompanied by the build up of an ice ridge consisting of ice blocks, broken from the edge of the floe. The average velocity of the ice blocks in a ridge is practically equal to zero but the velocity of the moving ice field is non-zero. Suppose the  $x$  coordinate is measured from the wall and the ridge occupies a domain of length  $L_r$  near the wall. We shall call the size of the wall along the  $y$  axis, which is perpendicular to the horizontal  $x$  axis and the vertical  $z$  axis, the width of the wall  $w_r$ . We will consider the ice cover as a two-dimensional continuum in the  $(x,y)$  horizontal plane, a description of which is possible within the framework of a plane stress state, and we will consider a ridge as a discontinuity line possessing intrinsic distributive dynamic characteristics: density per unit length, momentum and energy. The projection of the velocity of the ice particles onto the  $x$  axis, averaged over the ice thickness, changes on passing across the ridge boundary  $x=L_r$  from  $v$  (the velocity of the ice floe) to zero (the velocity of the ice blocks in the ridge). We can represent a ridge by a line when the ratio of the change in the width of the ridge  $L_r$  at a distance  $w_r$  to the width of the wall  $w_r$  is small. The assumption that the energy of the elastic strains is small composed with the energy dissipation as a consequence of friction is usually satisfied when ice interacts with wide structures.<sup>4</sup> It is further assumed that the formation of a ridge proceeds in a like manner in all the vertical sections of the ridge parallel to the  $(x, z)$  plane. In this case, the total ice load on the wall is equal to the product of the load per unit length on the wall from a segment of the ridge of unit length and the width of the wall  $w_r$ .

The per unit length density of the broken ice in the ridge is equal to  $\rho_i U_r$ , where  $\rho_i$  is the concentration of the ice and  $U_r$  is the area of the ice filling the cross-section of the ridge, where

$$U_r = \int_{-L_r}^0 \int_{z^-}^{z^+} \gamma dz dx \tag{1.1}$$

$z = z^+(x)$  and  $z = z^-(x)$  are the equations of the upper and lower surfaces of the ridge and  $\gamma$  is the concentration of the ice blocks in the ridge. The width of the ridge  $z = z^-(x)$  and the area of the ice in a cross-section of the ridge  $U_r$  increase during ridging. The momentum and kinetic energy of the ridge are equal to zero, since it is assumed that the velocity of the ice blocks in the ridge is equal to zero. The potential energy of the ridge, normalized to unit length of the ridge, is given by the formula ( $\rho_w$  is the density of water)

$$\Pi_r = \int_{-L_r}^0 \left[ \rho_i g \int_{z^-}^{z^+} \gamma z dz - \rho_w g \int_{z^-}^0 \gamma z dz \right] dx \tag{1.2}$$

In the one-dimensional case, the mass, momentum and total energy balance equations of the ice cover, integrated over the width of the ridge, have the form<sup>3</sup>

$$\frac{dU_r}{dt} - qh = 0, \quad -\rho_i q v h = \sigma_{xx}|_{x=0} - \sigma_{xx}|_{x=-L_r}, \quad \frac{d(\Pi_r + D_r)}{dt} - q\Pi = -v\sigma_{xx}|_{x=-L_r} \tag{1.3}$$

where  $q = v + dL_r/dt$  is the flux of flat ice into the ridge,  $h$  is the ice floe thickness which is piling up on the wall,  $\sigma_{xx}$  are the internal stresses, integrated over the thickness of the ice,  $dD_r/dt \geq 0$  is the rate of energy dissipation within the ridge and  $\Pi = \delta \rho_i g h^2 / 2$  is the surface potential energy density of the flat ice ( $\delta = (\rho_w - \rho_i) / \rho_w$ ).

Putting  $\rho_i = 920 \text{ kg/m}^3$  and  $v = 0.1 \text{ m/s}$ ,  $|q| \approx |v|$  and  $h = 1 \text{ m}$ , we find the estimate  $\rho_i h |qv| \approx 10 \text{ Pa.m}$ . The level of the ice loads on the wall can be far higher hence it follows from the second equation of (1.3), with a high degree of accuracy, that  $\sigma_{xx}|_{x=0} = \sigma_{xx}|_{x=-L_r} = -\sigma$ , where the quantity  $\sigma$  is the ice load on the wall per unit length.

In accordance with the general laws of thermodynamics, we define the rate of energy dissipation as the product of the flux of material into the ridge and the generalized force  $\sigma_d$  (with dimension of N/m)

$$dD_r/dt = q\sigma_d \tag{1.4}$$

Eliminating  $v$  from the first and last equations of (1.3) and using formula (1.4), we obtain the following expression for the ice load on the wall per unit length

$$\sigma = \left( h \frac{d\Pi_r}{dU_r} + \sigma_d - \Pi \right) \left( 1 - h \frac{dL_r}{dU_r} \right)^{-1} \tag{1.5}$$

It follows from formula (1.5) that the dependence of the load  $\sigma$  on the velocity of the ice floe is completely defined by the dependence of  $\sigma_d$  on  $v$ . Scenarios for the formation of a ridge in which  $\sigma_d$  is independent of  $v$  are considered next.

### 2. Scenarios for the ridging of ice near a fixed wall

A scenario for the formation of a ridge, based on observations during the course of experiments in an ice tank,<sup>5</sup> is shown in Fig. 1. In this scenario, an ice floe presses the ridge up to the wall, its fragments are raised along the wall and roll down onto the lateral surface  $BS_4$  of the sail of the ridge. The part of the ridge which is above waterline, which coincides with the  $x$  axis is called the sail of the ridge, and the part which is below waterline is called the keel. The interaction of the ice with the wall has a cyclic form. In this case, each cycle of the interaction between the ice and the wall can be arbitrarily divided into two stages. In the first stage, the sail of the ridge is constructed while the keel does not change, and fragments of the impressed ice floe move along the broken trajectory  $ABS_2S_3S_4$ . In the second stage, there is a break up of the ridge sail into the water, and a sharp fall in the ice load on the wall is observed. The physical reason of the caving in of the ridge sail is not completely understood. It has been suggested that it could be associated with losses in the bearing capacity of the ice floe which is forced into the ridge.<sup>5</sup>

We will assume that the wall has the shape of the broken line  $S_1S_2S_3S_4$  in Fig. 1a. In Fig. 1b, the boundary of the ridge sail is approximated by the broken line  $BS_4S_3S_2$ , and the keel is approximated by the triangle  $AS_2S_1$ . In the approach being used here, the shape of a ridge is defined by a six-order vector  $\chi = (h_s, h_k, h_w, \varphi_s, \varphi_k, \varphi_w)$ , where  $h_s$  and  $h_k$  are the height of the sail and the depth of the keel, and the quantities  $h_w$  and  $\varphi_w$  define the shape of the wall in the region of its contact with the ridge. It is assumed that the slope of the sail  $\varphi_s$  and the slope of the keel  $\varphi_k$  remain unchanged as the ice floe moves onto the wall and that the height of the sail  $h_s$  and the depth of the keel  $h_k$  increase.

The area of the ice which fills a cross-section of the ridge is bounded by the broken line  $ABS_4S_3S_2S_1$  (Fig. 1b) and is equal to the sum of the area of the vertical sections of the sail ( $U_s$ ), the keel  $\Pi_k$  and the segments of the impressed ice floe  $AS_2(U_1)$ ,  $S_2S_3(U_2)$  and  $S_3S_4(U_3)$ . The quantities  $U_s$ ,  $U_k$ ,  $U_f$  and  $U_i (i=1,2,3)$  are defined within quantities to  $O(h/L_r)$  by the formulae

$$\begin{aligned} U_s &= \frac{\gamma_s}{2} \left( \frac{h_s^2}{\text{tg } \varphi_s} - \frac{h_w^2}{\text{tg } \varphi_w} \right), & U_k &= \frac{\gamma_k h_k L_r}{2}, & U_1 &= h L_r, & U_2 &= \frac{h h_w}{\sin \varphi_w}, & U_3 &= h(h_s - h_w) \\ L_r &= h_k \left( \frac{1}{\text{tg } \varphi_k} + \frac{1}{\text{tg } \varphi_w} \right), & L_s &= \frac{h_s}{\text{tg } \varphi_s} - \frac{h_w}{\text{tg } \varphi_w} \end{aligned} \tag{2.1}$$

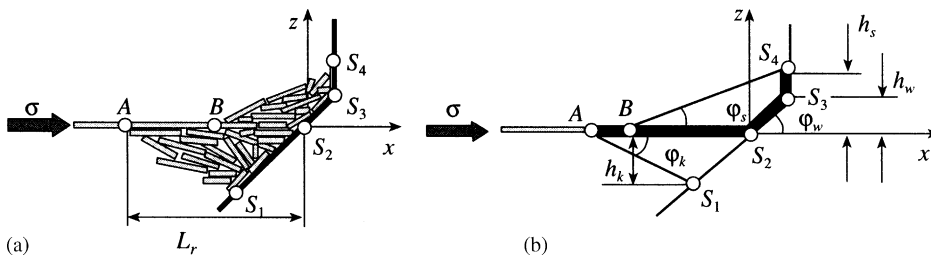


Fig. 1.

where  $L_r$  and  $L_s$  are the width of the ridge and the sail of the ridge, and  $\gamma_s$  and  $\gamma_k$  are the concentrations of the ice filling of the sail and keel.

The potential energy density per unit length of the ridge is equal to the sum of the potential energies of the sail  $\Pi_s$ , of the keel  $\Pi_k$  and of the impressed ice floe  $\Pi_f$ . Using formula (1.2), the quantities  $\Pi_s$ ,  $\Pi_k$  and  $\Pi_f$  can be written with accuracy  $O(h/L_r)$  in the form

$$\begin{aligned} \Pi_s &= \frac{\rho_i g \gamma_s}{6} \left( \frac{h_s^3}{\operatorname{tg} \varphi_s} - \frac{h_w^3}{\operatorname{tg} \varphi_w} \right), & \Pi_f &= \frac{\rho_i g}{2} \left( \frac{\delta h^2 h_k}{\operatorname{tg} \varphi_w} + \frac{h h_w^2}{\sin \varphi_w} + h(h_s^2 - h_w^2) \right) \\ \Pi_k &= \frac{(\rho_w - \rho_i) g \gamma_k h_k^3}{6} \left( \frac{1}{\operatorname{tg} \varphi_k} + \frac{1}{\operatorname{tg} \varphi_w} \right) \left( 1 + \frac{3h}{h_k} \right) \end{aligned} \tag{2.2}$$

### 3. Energy dissipation characteristics accompanying the ridge build up

We will denote the forces applied to the ice floe pressed into the ridge by  $R_j^\pm$  ( $j = 1, 2, 3$ ) (Fig. 2, a, b). The subscripts 1, 2 and 3 correspond to the fragments of the ice floe  $AS_2$ ,  $S_2S_3$  and  $S_3S_4$ . The forces applied to the surface of fragments by the sail are given a plus superscript, and the forces applied to the surface of the fragment  $AS_2$  by the keel ( $j = 1$ ) and to the surfaces of the fragments  $S_2S_3$  and  $S_3S_4$  ( $j = 2, 3$ ) by the wall are given a minus superscript. We now expand the reaction forces into normal and tangential components

$$\mathbf{R}_j^\pm = R_{n,j}^\pm \mathbf{n}_j + R_{\tau,j}^\pm \boldsymbol{\tau}_j \tag{3.1}$$

The normal unit vectors and the unit vectors tangential to the surfaces of the fragments of the impressed ice floe are defined by the formulae (Fig. 2a)

$$\begin{aligned} \mathbf{n}_1 &= (0, 1), & \boldsymbol{\tau}_1 &= (1, 0), & \mathbf{n}_2 &= (-\sin \varphi_w, \cos \varphi_w), \\ \boldsymbol{\tau}_2 &= (\cos \varphi_w, \sin \varphi_w), & \mathbf{n}_3 &= -\boldsymbol{\tau}_1, & \boldsymbol{\tau}_3 &= \mathbf{n}_1 \end{aligned} \tag{3.2}$$

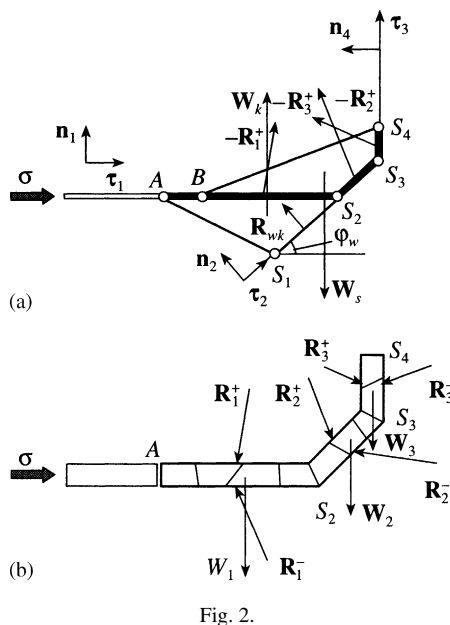


Fig. 2.

The generalized friction force  $\sigma_d$  is equal to the sum of the absolute values of the friction forces applied to the surfaces of the fragments  $AS_2$ ,  $S_2S_3$  and  $S_3S_4$  and is defined by the formula

$$\sigma_d = \sum_{j=1}^3 |R_{\tau,j}^+ + R_{\tau,j}^-| \tag{3.3}$$

We now write the balance of forces applied to the sail and the keel of the ridge in the form

$$\mathbf{W}_s - \mathbf{R}_1^+ - \mathbf{R}_2^+ - \mathbf{R}_3^+ = 0, \quad \mathbf{W}_k - \mathbf{R}_1^- + \mathbf{R}_{wk} = 0 \tag{3.4}$$

where  $\mathbf{W}_s = (0, -\rho_i g U_s)$  is the weight of the sail and  $\mathbf{W}_k = (0, (\rho_w - \rho_i) g U_k)$  is the sum of the weight of the keel and the buoyancy force, while  $\mathbf{R}_{wk} = r_{wk} \mathbf{n}_2$  is the reaction force applied to the keel by the segment of the wall  $S_1S_2$ , and it is assumed that this force is directed along the normal to the wall.

We shall assume that the Coulomb - Mohr condition for dry friction is satisfied on the contact surfaces between the impressed ice floe and the sail and the wall

$$\begin{aligned} R_{\tau,j}^+ &= \mu_{ii} R_{n,j}^+, \quad (j = 1, 2, 3); \quad R_{\tau,1}^- = -\mu_{ii} R_{n,1}^-, \\ R_{\tau,2}^- &= -\mu_{iw} R_{n,2}^-, \quad R_{\tau,3}^- = -\mu_{iw} R_{n,3}^- \end{aligned} \tag{3.5}$$

where  $\mu_{ii}$  and  $\mu_{iw}$  are the friction coefficients of ice with ice and ice with the wall.

It is assumed that the normal projections of the forces  $R_{n,j}^-$  ( $j = 2, 3$ ) applied to the surfaces of the fragments of the ice floe are related to the weights of the corresponding fragments by the formulae

$$(\mathbf{R}_j^- + \mathbf{R}_j^+ + \mathbf{W}_j) \cdot \mathbf{n}_j = 0, \quad j = 2, 3 \tag{3.6}$$

The weights of the fragments of the impressed ice floe are equal to  $\mathbf{W}_j = (0, -\rho_i g U_j)$ . Terms corresponding to the normal projections of the interaction of the fragments of the ice floe applied to the end faces of the fragments have been omitted in Eq. (3.6). This was done on the assumption that there is a narrow layer between the end faces of the fragments which is filled with crumbly broken ice which transmit pressure well and significantly lowers the friction. It is therefore assumed that the pressure on the end faces of the fragments normal to the vectors  $\mathbf{n}_j$  does not make any contribution to Eq. (3.6).

In scalar form, the 12 Eqs. (3.4)–(3.6) contain 15 quantities which change during the ridging of ice near a wall: 12 components of the vectors  $\mathbf{R}_j^\pm$ , the reaction force  $r_{wk}$ , the sail height  $h_s$  and the keel depth  $h_k$ . We now formulate two additional relations which enable us to express that ice load per unit length on the wall (1.5) in terms of a single parameter, for example, the sail height in the form

$$\sigma = \left( h \frac{d\Pi_r}{dh_s} \left( \frac{dU_r}{dh_s} \right)^{-1} + \sigma_d - \Pi \right) \left( 1 - h \frac{dL_r}{dh_s} \left( \frac{dU_r}{dh_s} \right)^{-1} \right)^{-1} \tag{3.7}$$

The additional relations have been formulated using an idealization of the ridging process, and the resulting expressions for the load of the ice on the wall cannot therefore describe in detail the actual relations obtained in laboratory and natural experiments. At the same time, they are useful for estimating ice loads.

The equilibrium conditions (3.4) and formulae (3.5) determine the reaction forces acting on the sail of a ridge of specified dimensions, apart from a constant quantity. As a criterion for the choice of the unique solution, it is proposed to use an additional hypothesis concerning the minimality of the friction stresses on the surfaces of the fragments of the impressed ice floe, according to which the quantity

$$Z = \sum_{j=1}^3 (R_{\tau,j}^+ + R_{\tau,j}^-)^2 \tag{3.8}$$

reaches a minimum in the case of the actual motion, that is, the condition

$$\partial Z / \partial R_{n,1}^+ = 0 \tag{3.9}$$

is satisfied, where the derivative is calculated after substituting the solution of Eqs. (3.4)–(3.6) into expression (3.8).

During the formation of the sail of the ridge when the keel remains unchanged, it is assumed that

$$h_k = \text{const} \tag{3.10}$$

The break up of the impressed ice floe can lead to the balance between the gravitational and buoyancy forces acting on its fragment  $AS_2$ , i.e.

$$R_{n,1}^+ + R_{n,1}^- + (\rho_w - \rho_i)gU_1 = 0 \tag{3.11}$$

The last term on the left-hand side of relation (3.11) is equal to the sum of the weight and the buoyancy force of the fragment  $AS_2$ . It is assumed that the fragment  $AS_2$  is located in a trampled position after the break up of the ice floe. In a similar way to the assumptions made when formulating Eq. (3.6), the vertical projection of the force applied to the end of a fragment at the point  $S_2$  is assumed to be small and is not taken into account in Eq. (3.11).

We propose to use Eqs. (3.9) and (3.10) as the two additional conditions for finding the upper limit of the ice load on the wall and to use Eqs. (3.9) and (3.11) to find the lower limit. If the inclination of the wall is constant, it is necessary to put  $R_3^\pm = 0$  in Eq. (3.4). In this case, the vectors  $R_1^\pm$  and  $R_2^\pm$  are uniquely determined from Eqs. (3.4)–(3.6)

$$\begin{aligned} R_{1,x}^\pm &= \pm \mu_{ii} R_{1,z}^\pm, & R_{1,z}^+ &= -W_s \frac{1 - \mu_{ii} \text{ctg} \varphi_w}{1 + \mu_{ii}^2}, & R_{2,x}^+ &= -R_{1,x}^+, & R_{2,z}^+ &= -W_s \mu_{ii} \frac{\mu_{ii} + \text{ctg} \varphi_w}{1 + \mu_{ii}^2} \\ R_{1,z}^- &= (\rho_w - \rho_i)gU_k, & R_{2,z}^- &= -\frac{(\mu_{iw} - \text{ctg} \varphi_w)(2W_s \mu_{ii} + W_2 \sin(2\varphi_w)(1 + \mu_{ii}^2))}{2(1 + \mu_{ii}^2)} \\ R_{2,x}^- &= -\frac{1 + \mu_{iw} \text{ctg} \varphi_w}{\mu_{iw} - \text{ctg} \varphi_w} R_{2,z}^-, & W_s &= \rho_i g U_s, & W_2 &= \rho_i g U_2. \end{aligned} \tag{3.12}$$

It is assumed in formulae (3.12) that  $\text{tg} \varphi_w > \mu_{ii}$ . When this condition is not satisfied, the broken ice does not slide down along the ice floe which is forced onto the wall. From formulae (3.12), it follows that  $R_{n,2}^- > 0$  and  $R_{\tau,2}^- < 0$ .

**4. The criterion for the formation of a flexural crack**

In order to formulate a criterion for the break up of an ice floe, we will consider the problem of the buckling of a semi-infinite elastic plate on a hydraulic foundation under distributed load. The deviation of points of the plate from the horizontal position  $\eta(x)$  is described by the equation

$$D \frac{d^4 \eta}{dx^4} + \rho_w g \eta = P, \quad x < 0; \quad D = \frac{Eh^3}{12(1 - \nu^2)} \tag{4.1}$$

where  $D$  is the stiffness of the plate,  $h$  is the thickness and  $E$  and  $\nu$  are Young’s modulus and Poisson’s ratio of the ice. The diagram of a distributed load is shown in Fig. 3. The points  $A$  and  $B$  have the coordinates  $-L_r$  and  $-L_s$  on the  $x$  axis and the value of  $x_0 = h_k \text{ctg} \varphi_w$  is equal to the coordinate of the point  $S_1$  in Fig. 1. The distributed load per unit length  $P = P_s + P_k$  is determined by the reaction forces applied to the fragment of the ice floe  $AS_2$  by the sail and the

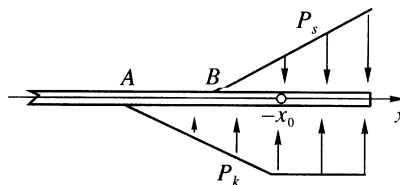


Fig. 3.

keel and is modelled by the formulae

$$P_s = 2R_{n,1}^+ \frac{L_s + x}{L_s^2}, \quad x \in (0, -L_s); \quad P_k = 2R_{n,1}^- \begin{cases} (L_r + x_0)^{-1}, & x \in (0, -x_0) \\ (L_r^2 - x_0^2)^{-1} (L_r + x), & x \in (-x_0, -L_r) \end{cases} \quad (4.2)$$

The width of the ridge  $L_r$  and of the ridge sail  $L_s$  are given by formulae (2.2). The equalities

$$R_{n,1}^+ = \int_0^{-L_s} P_s dx, \quad R_{n,1}^- = \int_0^{-L_r} P_k dx$$

follow from formulae (4.2).

It is assumed that, at considerable distances from the wall, the ice floe is not buckled by external forces and, close to the wall, the bending moment acting on the edge of the ice floe is equal to zero:

$$\eta \rightarrow 0, \quad x \rightarrow -\infty; \quad \frac{d^2 \eta}{dx^2} = 0, \quad x = 0 \quad (4.3)$$

In addition to conditions (4.3), one of the following boundary conditions is considered on the edge of the ice floe

$$\eta = 0, \quad x = 0 \quad (4.4)$$

$$\frac{d^3 \eta}{dx^3} = 0, \quad x = 0 \quad (4.5)$$

Condition (4.4) is satisfied when the edge of the impressed ice floe is supported by the wall. Condition (4.5) corresponds to the case when the ice floe edge is located close to the wall and does not touch it.

We will call the solutions of Eq. (4.1) which satisfy conditions (4.3) and (4.4), solutions of class I and those which satisfy conditions (4.3) and (4.5) solutions of class II.

The criterion for the formation of a flexural crack in an ice floe reduces to the equality of the total tensile force  $\sigma_t$  on the ice floe surface to the tensile strength of the ice  $\sigma_{cr}$ . The tensile stress on the ice floe surface accompanying bending is equal to  $\sigma_{xx}^{3D} = 6|M|h^{-2}$ , where  $M = Dd^2\eta/dx^2$  is the bending moment. The total stress  $\sigma_t$  on the ice floe surface as a result of bending in the case of a compressive load  $\sigma$  is equal to  $\sigma_{xx}^{3D} - \sigma h^{-1}$ . Hence, the criterion for the formation of a flexural crack is written in the form

$$\max_{x>0} |M| = (\sigma_{cr} + \sigma h^{-1})h^2/6 \quad (4.6)$$

When the sail and the keel are small, the distributed load per unit length on the ice floe is insufficient to satisfy criterion (4.6). For a given size of the keel, criterion (4.6) is satisfied when the height of the sail reaches a critical value which depends on the size of the keel. A flexural crack is then formed in the ice floe. Note that the ice retains its bearing capacity for quite a long time even after the final development of flexural cracks,<sup>6</sup> and hence the collapse of the sail of the ridge may set in when its dimensions are considerably greater.

### 5. Ice loads on a wall

The results of calculations of the ridging of ice near a wall in an experiment in an ice tank are shown in Figs. 4–6. In the experiment, an ice floe of thickness  $h = 35$  mm, which had been artificially prepared, moved with a velocity  $v = 13.5$  cm/s onto a wall of width  $w_r = 1.75$ , a height above the water level  $h_w = 80$  and an angle of inclination  $\varphi_w = 58^\circ$ . The ice - ice and ice - wall friction coefficients were  $\mu_{ii} = 0.35$  and  $\mu_{iw} = 0.15$ . The measured values of Young’s modulus and the bending strength of the ice were about  $E = 5 \times 10^7$  N m<sup>-2</sup> and  $\sigma_f = 20$  kPa. In the calculations it was assumed that  $\varphi_s = \varphi_k = 30^\circ$ ,  $\gamma_s = 0.8$ ,  $\gamma_k = 0.7$  and  $\sigma_{cr} = \sigma_f$ .

The total ice load on the wall measured in the experiment is shown by the solid line in Fig. 4, and the results of the calculations are shown by the dashed lines. The line  $L_{\min}$  shows the lower limit of the ice load, calculated using assumption (3.11) concerning the hydrostatic equilibrium of the sail, the keel and the fragment  $AS_2$  of the ice floe which

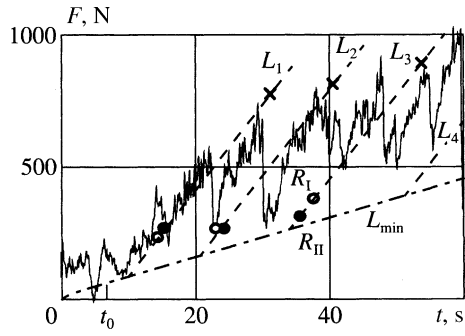


Fig. 4.

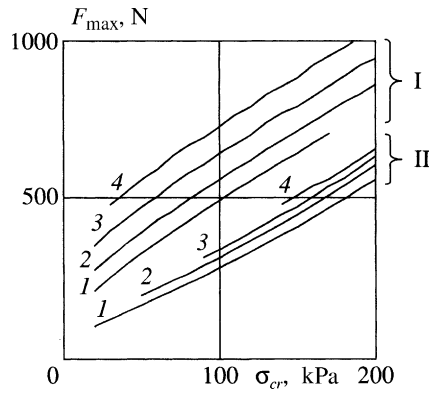


Fig. 5.

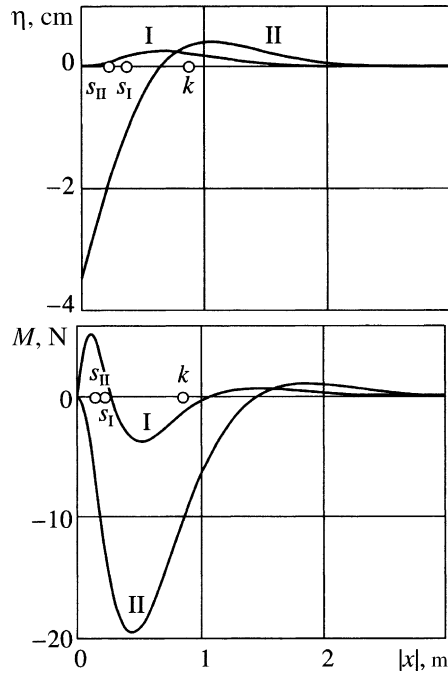


Fig. 6.



is being impressed (Fig. 1). The calculated lines  $L_1, \dots, L_4$  were constructed using assumption (3.10) that the size of the keel is constant; this dimension is constant for each of the calculated lines and is determined by the dimension of the keel corresponding to the point of intersection with the line  $L_{\min}$ . The height of the sail reaches a value of  $h_w = 80$  mm at the instant of time  $t_0 = 6.3$  s and the broken line shape of the wall begins to have an effect on the process.

The dependences of the ice loads  $F_{\max}$ , which arise at the instant a flexural crack forms, on the tensile strength of the ice  $\sigma_{cr}$  when  $20 \text{ kPa} < \sigma_{cr} < 220 \text{ kPa}$  are shown in Fig. 5. Curves 1, 2, 3, and 4 were constructed for keel sizes corresponding to the lines  $L_1, L_2, L_3, L_4$ . The groups of curves I and II were constructed for solutions of class I and II of Eq. (4.1). Almost all the curves begin or terminate at a fixed value of the strength  $\sigma_{cr}$ . The constraint on curves to the left means that, for smaller values of the strength  $\sigma_{cr}$ , an ice floe is already broken by bending in the case of the equilibrium form of a ridge at points of the line  $L_{\min}$ . As the number of the line becomes larger, the dimensions of the ridge increase and the distributed load on the ice floe increases. Lines with larger numbers therefore begin at larger values of  $\sigma_{cr}$ . The constraint on the curves to the right means that, at large values of the strength  $\sigma_{cr}$ , the ice floe is broken by bending when the width of the sail exceeds the width of the keel:  $L_s > L_r$ . The calculation was only carried out for the case when  $L_s < L_r$ . It can be seen from Fig. 5 that the ice load on the wall at the instant a flexural crack occurs in the ice floe is significantly greater in cases when the ice floe edge is supported on the wall. An increase in the strength of the ice floe  $\sigma_{cr}$  leads to an almost linear increase in the ice loads. The values of the load on the wall at the instant a flexural crack occurs during the stage when the sail is being formed while the keel is unchanged, the size of which corresponds to the lines  $L_1, L_2$  and  $L_3$ , are labelled with the open and filled circles and small crosses in Fig. 4. The open circles and crosses correspond to solutions of class I and an ice strength  $\sigma_{cr} = 20 \text{ kPa}$  and  $\sigma_{cr} = 190 \text{ kPa}$  while the filled circles correspond to a solution of class II and a strength  $\sigma_{cr} = 90 \text{ kPa}$ .

The form of the flexure of the ice floe  $\eta$  and the bending moments  $M$  which arise in it at the instant a fissure occurs under the action of the distributed load are shown in Fig. 6. Curves I and II correspond to the classes of solutions I and II of Eq. (4.1) and were constructed for dimensions of the sail and the keel corresponding to the points  $R_I$  and  $R_{II}$  in Fig. 4. The point  $k$  shows the boundary of the keel of the ridge and the points  $S_I$  and  $S_{II}$  show the boundary of the sail. In solution I, the ice floe edge lies on the wall. The maximum bending moment occurs within the limits of the sail of the ridge. In solution II, the ice floe edge sags down by approximately 3.5 cm close to the wall. It is obvious that the wall will impede such a displacement. However, it can be assumed that the solution will have an analogous form if the ice floe edge does not quite reach the wall. The maximum flexural moment occurs within the keel of the ridge.

Calculations of the ridging of the ice close to the wall, the dimensions of which correspond to real ice-resistant platforms, are shown in Figs. 7 and 8. In the calculations, it is assumed that ice of thickness  $h = 1$  m moves with a velocity  $v = 13 \text{ cm/s}$  against a wall of width  $w_r = 105$  m. The height of the wall above the water level  $h_w = 4.8$  and its inclination  $\varphi_w = 58^\circ$ . The ice - ice and ice - wall friction coefficients were  $\mu_{ii} = 0.35$  and  $\mu_{iw} = 0.2$ . It is assumed that  $\varphi_s = \varphi_k = 30^\circ$ ,  $\gamma_s = 0.8$  and  $\gamma_k = 0.7$ . A value of Young's modulus  $E = 3 \times 10^9 \text{ N/m}^2$  was used when calculating the bending. In the upper part of Fig. 7, the line  $L_{\min}$  shows the lower bound of the ice load calculated using assumption (3.11) concerning the hydrostatic equilibrium of the sail, the keel and the fragment of the impressed ice floe  $AS_2$ . The

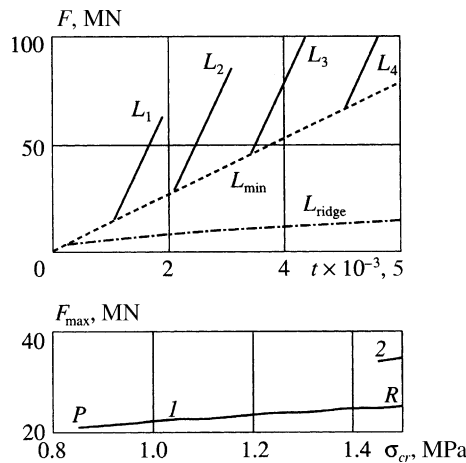


Fig. 7.

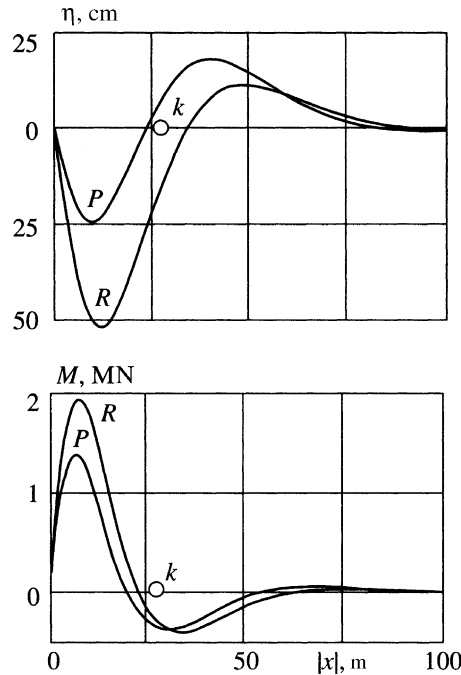


Fig. 8.

lines  $L_1, \dots, L_4$  were constructed using assumption (3.1) concerning the constancy of the keel size. The keel size is constant for each of these lines and is determined by the keel size at the point of intersection with the line  $L_{min}$ . At the instant of time  $t = 11.6$  min the height of the sail reaches a value  $h_w = 4.8$  and the broken line form of the wall starts to have an effect on the process.

Calculations show that the action of the distributed load, in the case of the equilibrium dimensions of the sail and the keel corresponding to the curve  $L_{min}$ , leads to breakdown of the ice floe by bending when its shape is described by solutions of class II. The dependences of the maximum ice loads, corresponding to the instant a flexural crack occurs within the framework of the solutions of class I, on the tensile strength of the ice  $\sigma_{cr}$  when  $0.5 \text{ MPa} < \sigma_{cr} < 1.5 \text{ kPa}$  are shown in the lower part of Fig. 7. The above range of variation in  $\sigma_{cr}$  corresponds to the flexural strength of ice calculated on the basis of experiments with sea ice.<sup>7</sup> Curves 1 and 2, constructed for keel dimensions which correspond to the lines  $L_1$  and  $L_2$ , begin at a fixed value of the strength  $\sigma_{cr}$ . At lower values of the strength an ice floe is fractured by bending in the case of the equilibrium form of the ridge at points of the line  $L_{min}$  when the bending of the ice floe is described by solutions of class I. An increase in the ridge dimensions and the distributed load on the ice floe correspond to an increase in the number of the curve. At sufficiently large equilibrium dimensions of the sail and the keel (which correspond, for example, to the initial points of the lines  $L_3$  and  $L_4$ ) the ice floe fractures for any value of the strength  $\sigma_{cr}$  from the range of values being considered. The maximum ice load on the wall at the instant fracture of the ice floe occurs insignificantly exceeds the load in the case of the equilibrium form of the ridge at points of the curve  $L_{min}$ .

The form of an ice floe, which is described by solutions of class I of Eq. (4.1), and the bending moments  $M$  which arise in the ice floe at the instant a crack occurs are shown in Fig. 8. Curves  $p$  and  $R$  were constructed for the dimensions of the sail and the keel corresponding to the points  $P$  and  $R$  in the lower part of Fig. 7 (the points  $P$  and  $R$ , which are not shown in the upper part of Fig. 7, are located close to the point of intersection of the lines  $L_1$  and  $L_{min}$ ). The point  $k$  shows the boundary of the ridge keel. The width of the sail is equal to 7.1 m at point  $P$  and 8 m at point  $R$ . It is seen that the maximum bending moment occurs close to the edge of the sail.

The line  $L_{ridge}$  in the upper part of Fig. 7 corresponds to the relation<sup>8</sup>

$$\sigma = kh\sqrt{U_r}, \quad k = \rho_i g \left( \frac{\sqrt{\text{tg}\theta}}{2(1 + \kappa^2)^{3/2}} \left( \frac{\rho_w - \rho_i}{\rho_i} \kappa^3 + 1 \right) + \frac{\mu_{ii}\kappa}{\sqrt{(1 + \kappa^2)\text{tg}\theta}} \right) \quad (5.1)$$

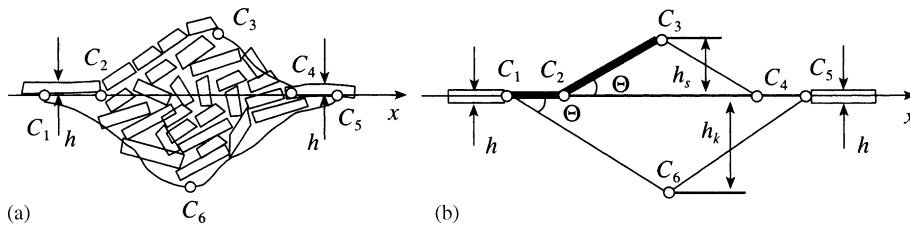


Fig. 9.

The stress per unit length (5.1) was obtained for the scenario of the formation of a ridge of isosceles triangles  $C_2C_3C_4$  and  $C_1C_6C_5$ , with identical slopes  $\theta = 30^\circ$ , which represent the sail and the keel of the ridge. In this case, the area of the vertical section of the ridge was calculated using the formula  $U_r = h_s^2(1 + \kappa^2)\text{ctg}\theta$ , where the parameter  $\kappa = h_k/h_s$  was put equal to 4.4. In the scenario being considered, energy dissipation occurs as a result of the friction between the fragments of the ice floe, which advance along the lateral surface of the sail  $C_1C_2C_3$ , and the surface of the sail (Fig. 9, b). It is clear that the loads accompanying the ridge build up close to the wall significantly exceed the load accompanying the ridge build up between ice floes.

## 6. Conclusion and results

The ice load, calculated using the assumption of the hydrostatic equilibrium of the sail and the keel of a ridge, indicates the lower boundary of ice loads on the wall measured in experiments in an ice tank. The upper limit of the calculated ice loads, obtained using the assumption of the constant size of the ridge keel, increases without limit as the size of the ridge sail increases. In this case, the real level of the maximum loads is determined by the instant when the ridge collapses into the water. For a specified keel size, the calculated loads, which occur at the instant a flexural crack occurs in the ice floe which is moving onto the wall, have a level of the experimentally measured maximum loads for values of the flexural strength of the ice which are an order of magnitude greater than the experimentally measured values of the strength. The calculated ice loads on the wall at the instant a flexural crack occurs are approximately half the maximum experimentally measured loads for real values of the flexural strength. It is possible that this is related to the fact that a loss of bearing capacity of the ice floe which maintains the sail sets in much later than the occurrence of a flexural crack. The ice loads accompanying the motion of an ice layer of thickness 1 m onto a wall of length 105 m was calculated for the case of cyclic interaction with the wall, which had been observed in a laboratory experiment. The form of the wall is similar to the form of the wall in the experiment. The tensile strength of the ice sheet corresponded to the flexural strength of sea ice. It was found that the calculated ice loads, arising at the instant a flexural crack occurred in the ice floe which supports the sail of the ridge, are close to the ice loads obtained using the assumption of the hydrostatic equilibrium of the sail and the keel of the ridge. The ice load per unit length of wall reached a value of 0.76 MPa m in calculations for a height of the sail of 13 m and a depth of the keel of 27 m. Assuming that the maximum ice load per unit length of the wall is twice as great, we obtain an estimate of 1.5 MPa.m for it. The loads necessary for a ridge to form between two ice floes are much smaller and, when an ice field drifts onto a platform, it is therefore natural to assume that ridges form at a certain distance from it, at places where the ice cover has been weakened by cracks, for example.

In the ridging scenarios which have been considered, kinematically permissible schemes for the motion of the ice close to the wall are used, which are qualitatively different from the classical schemes based on the Prandtl solution regarding the indentation of a punch in which plastic deformation of the medium occurs as a result of the displacements of domains of triangular shape. The direct use of classical schemes in problems on the ridges build up has not been completely substantiated since the number of blocks of ice constituting a ridge is not sufficiently large and a ridge cannot be considered as an analogue of a granular material such as sand or gravel. At the same time, it can be assumed that, as time passes, the rheological properties of a ridge approximate to those of a granular material<sup>9</sup> and the use of classical approaches is therefore more justified in calculations of the action of preformed ridges on wide structures.<sup>10,11</sup>

## Acknowledgements

I wish to thank S.A. Vershinin, R.V. Goldstein, M.M. Karulina and Ye.B. Karulin for useful comments.

This research was supported by the Russian Foundation for Basic Research (05-01-00219) and the Support for the Leading Scientific Schools Programme (Nsh 4710.2006.1).

## References

1. Hopkins MA. Four stages of pressure ridging. *J Geophys Res* 1998;**103**(10):21883–91.
2. Croasdale KR, Cammaert AB, Metge M. A method for the calculation of sheet ice loads on sloping structures. In: *Int. Assoc. Hydraul. Res. Ice Symp.*. Norway: Trondheim; 1994. p. 874–85.
3. Marchenko AV. Models of the sea ice ridging. *Uspekhi Mekhaniki* 2002;**1**(3):67–129.
4. Ashton GD, editor. *River and Lake Ice Engineering*. Michigan, USA: Book Crafters; 1986. p. 485.
5. Alexeev YN, Karulina MM. A numerical prediction method for ice load on wide sloping offshore structures. In: Shen HT, editor. *Ice in Surface Waters*. Rotterdam: Balkema; 1998. p. 511–7.
6. Doronin YuP, Kheisin DE. *Sea Ice*. New Delhi: American Publishing Co. for the National Science Foundation; 1977.
7. Timco GW, Johnston ME. Sea ice strength during the melt season. *Ice in the Environment: Proc. 16th Int. Assoc. Hydraul. Res. Int. Symp. on Ice*. Dunedin, New Zealand: IAHR; 2002; **2**:187–93.
8. Marchenko A, Makshtas A. A dynamic model of ice ridge build up. *Cold Reg Sci and Tech* 2005;**41**(3):175–88.
9. Kioka S, Matuo Y, Kondo H, Yamamoto Y, Saeki H. Mechanical properties of unconsolidated layer model of ice ridge under various conditions. *Proc. 17th Intern. Symp. on Ice*. St. Petersburg: VNIIG; 2004;**1**:53–60.
10. Bekker AT, Komarova OA, Venkov AV. Distribution of extreme ice loads on ice resistant platforms. In: Shen HT, editor. *Ice in Surface Waters*. Rotterdam: Balkema; 1998. p. 469–74.
11. Vershinin SA, Truskov PA, Kouzmitchev KV. Impact of hummock formations on vertical structures. In: *Proc. OMAE04: 23rd Int. Conf. on Offshore Mechanics and Arctic Eng.* Canada: Vancouver; 2004. p. 51271.

Translated by E.L.S.